JACS
JOURNAL OF THE AMERICAN CHEMICAL SOCIETY
Communication
pubs.acs.org/JACS

Ribozyme–Spherical Nucleic Acids

Jessica L. Rouge,[†,‡,#] Timothy L. Sita,[§,‡,⊥,#] Liangliang Hao,[§,‡] Fotini M. Kouri,[‡,⊥,∥] William E. Briley,[§,‡] Alexander H. Stegh,[‡,⊥,∥] and Chad A. Mirkin*[,†,‡]

[†]Department of Chemistry, [‡]International Institute for Nanotechnology, and [§]Interdisciplinary Biological Sciences Graduate Program, Northwestern University, Evanston, Illinois 60208, United States

[⊥]The Brain Tumor Institute, The Robert H. Lurie Comprehensive Cancer Center, Northwestern University, Chicago, Illinois 60611, United States

[∥]Ken and Ruth Davee Department of Neurology, Feinberg School of Medicine, Chicago, Illinois 60611, United States

Supporting Information

ABSTRACT: Ribozymes are highly structured RNA sequences that can be tailored to recognize and cleave specific stretches of mRNA. Their current therapeutic efficacy remains low due to their large size and structural instability compared to shorter therapeutically relevant RNA such as small interfering RNA (siRNA) and microRNA (miRNA). Herein, a synthetic strategy that makes use of the spherical nucleic acid (SNA) architecture to stabilize ribozymes and transfect them into live cells is reported. The properties of this novel ribozyme–SNA are characterized in the context of the targeted knockdown of O^6-methylguanine-DNA methyltransferase (MGMT), a DNA repair protein involved in chemotherapeutic resistance of solid tumors, foremost glioblastoma multiforme (GBM). Data showing the direct cleavage of full-length *MGMT* mRNA, knockdown of MGMT protein, and increased sensitization of GBM cells to therapy-mediated apoptosis, independent of transfection agents, provide compelling evidence for the promising properties of this new chemical architecture.

Ribozymes are RNA sequences containing a highly conserved catalytic loop capable of cleaving mRNA.[1,2] Along with a high degree of sequence specificity for their substrates, ribozymes offer an attractive alternative to other therapeutic nucleic acid approaches, as they are able to directly cleave specific stretches of mRNA, rather than recruiting enzymes to mRNA for cleavage.[3,4] Ribozymes have therefore attracted significant attention as potential therapeutic gene-silencing agents.[5,6] However, one of the greatest hurdles preventing ribozymes from becoming a viable gene silencing modality is their susceptibility to chemical degradation and strict requirement for proper folding to recognize and cleave their intended substrate. Due to their relatively fragile structures, ribozymes are often delivered into cells only after extensive chemical modification and encapsulation in liposomes and block copolymers,[7] via assembly into larger RNA scaffolds,[8] or through plasmid-directed expression.[9,10]

The aforementioned approaches can be synthetically challenging and, depending on the ribozyme sequence, can cause substantially lower catalytic cleavage efficiencies.[11,12] Due to such hurdles, researchers have explored alternative approaches for targeting RNA substrates,[13] including larger RNA cleaving protein–nanoparticle conjugates. In an effort to develop a straightforward method of creating functional ribozyme structures, without having to undertake extensive chemical modification of the RNA, and ensure catalytic activity, we investigated the concept of incorporating a ribozyme into a spherical nucleic acid (SNA) architecture. SNAs are typically composed of spherical nanoparticles densely functionalized with oligonucleotides (either DNA or RNA), and they have been shown to increase nucleic acid stability in cellular environments by limiting the extent of degradation caused by endogenous nucleases.[14−17] Using an enzymatic ligation reaction,[18] a ribozyme can be covalently attached to a SNA surface without chemical changes introduced into the RNA's sequence. The resulting composite architecture combines the unique RNA structural stabilization properties offered by SNAs with the ribozyme's ability to target and catalytically cleave a specific mRNA sequence (Figure 1).

Such an approach provides the potential for the ribozyme's downstream biological function to be retained, as it is the ligase's sequence recognition that serves as the basis of assembly at the nanoparticle's surface rather than chemical modification of the ribozyme itself.

Herein we describe ribozyme–SNA conjugates that exhibit high cellular uptake, comparable to that observed for previous classes of SNAs,[21] and which allow the ribozyme to remain catalytically active and stable, as shown through a combination of *in vitro* RNA cleavage and RT-PCR assays, respectively.

The ribozyme sequence used for this study was designed to target the mRNA for O^6-methylguanine-DNA methyltransferase (MGMT). MGMT was chosen as a target for the ribozyme–SNAs due to its critical role in regulating therapy susceptibility of glioblastoma multiforme (GBM).[22] In GBM, a highly aggressive and uniformly deadly brain cancer, higher expression of MGMT protein has been linked to resistance to temozolomide (TMZ) therapy.[23] TMZ, an alkylating chemotherapeutic, induces apoptosis in cancer cells by methylating the O^6-position of guanine in DNA.[24] These O^6-methylguanine lesions can bind thymine rather than cytosine, leading to futile mismatch repair cycles and eventual apoptosis. When MGMT is present, it is able to repair O^6-methylguanine lesions induced

Received: July 8, 2015
Published: August 14, 2015

DOI: 10.1021/jacs.5b07104
J. Am. Chem. Soc. 2015, 137, 10528−10531

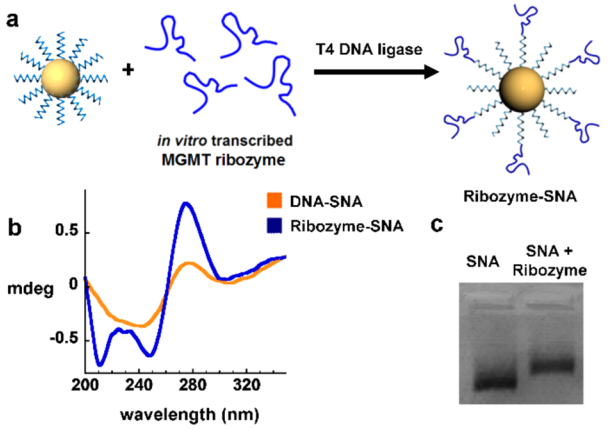

Figure 1. Assembly of ribozyme-SNAs using enzymatic ligation. (a) Schematic depicting the ligation approach for constructing ribozyme-SNAs. (b) Circular dichroism of ribozyme-SNAs. Orange trace showing B-form DNA at the SNA surface, as indicated by the maxima at 277 nm and the minima at 246 nm (broadening attributed to interactions with the gold nanoparticle surface[19]). The blue trace indicates the presence of an A form RNA sequence[20] at the particle surface, as indicated by the slightly blue-shifted peak at 275 nm, along with the minima at 210 nm. (c) Agarose gel shift assay showing the larger size of the gold nanoparticles post ligation and covalent attachment of the ribozyme to the SNA surface. Changes in particle size were also confirmed using dynamic light scattering (Table S2).

by TMZ, causing resistance and reducing overall clinical efficacy.[25] In order to sensitize GBM cells to TMZ-induced apoptosis, we sought to lower the expression of MGMT protein in glioma cells through ribozyme−SNA directed cleavage of *MGMT* mRNA.

The ribozyme sequence used in the construction of the ribozyme−SNAs was adapted from a truncated MGMT-targeting ribozyme designed by Citti and co-workers.[26] The sequence contains a hammerhead-type structure which, upon binding a divalent ion in its cleavage reaction site, cleaves an RNA bound to its recognition region.[27] All ribozymes used in this study were transcribed enzymatically, ligated to a DNA−SNA nanoconjugate,[18] and delivered to cells without auxiliary transfection agents.

In order to initially evaluate the ribozyme−SNA's ability to recognize and cleave the RNA transcript encoding MGMT, the ribozyme−SNAs were incubated with a short stretch (13 bases) of RNA derived from the full-length MGMT mRNA. The 13mer RNA substrate was modified at its 3′ end with a fluorescein and at its 5′ end with Cy5 for visualization of the cleaved products by gel electrophoresis. Next, 20 nM ribozyme−SNAs (carrying 20 ± 1 ribozymes per particle) were incubated with the 13mer RNA substrate overnight at 37 °C in the presence or absence of 40 mM $MgCl_2$, an essential cofactor for ribozyme-catalyzed cleavage. After 12 h, the ribozyme−SNAs were centrifuged and removed from the reaction, and the supernatant was run on a denaturing polyacrylamide gel to evaluate the extent of RNA cleavage.

As compared to the background degradation observed for the 13mer RNA substrate (Figure 2, first lane), it is evident that both the free ribozyme and the ribozyme−SNAs are capable of cleaving the intended substrate to a similar extent in a Mg^{2+}-dependent fashion. Therefore, the ribozyme−SNA is as effective as the free ribozyme in cleaving a 13mer RNA substrate *in vitro* (Figure 2), suggesting that the tertiary structure of the ribozyme is sufficiently retained post enzymatic

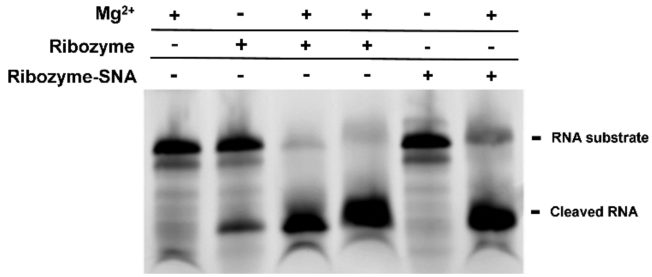

Figure 2. *In vitro* cleavage assay for ribozyme−SNAs: an 8% denaturing polyacrylamide gel indicating the cleavage of the ribozyme's RNA substrate under various conditions of salt and time. The 13mer RNA substrate is cleaved in the presence of the ribozyme−SNA when $MgCl_2$ is present. The third and fourth lanes differ in total incubation time, 12 h versus 24 h, respectively.

ligation. These data functionally confirm circular dichroism studies, which identified elements of a characteristic A-fold RNA sequence within the ribozyme−SNA (Figure 1b).

It was then investigated whether the ribozyme−SNA could successfully transfect cells much like native SNAs but in manner that retains its enzymatic activity. Using a Cy5 fluorophore-labeled ribozyme−SNA, it was shown that the ribozyme-tethered SNA could indeed enter cells, whereas a free Cy5-ribozyme showed insignificant uptake by cells (Figure 3).

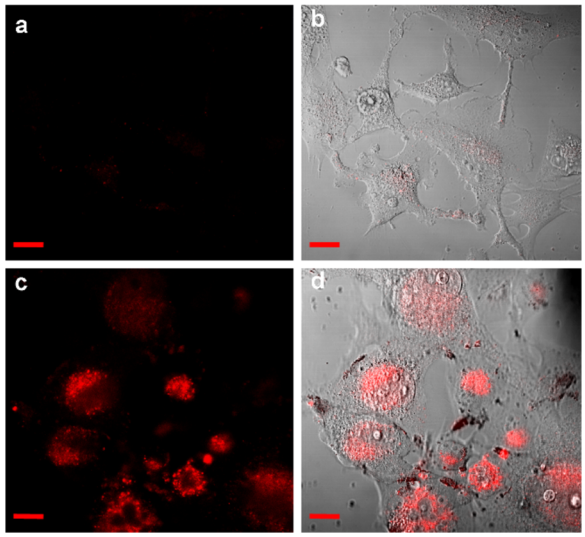

Figure 3. Confocal images of ribozyme-SNA uptake into T98G glioma cells. Comparison of cellular entry as a function of Cy5 emission for free Cy5-ribozymes versus Cy5-ribozyme−SNAs, indicating a greater degree of uptake for SNA-tethered ribozymes. (a) Cy5 channel for free ribozyme. (b) Bright-field images with Cy5 channel overlay showing T98G cells post incubation with free Cy5-labeled ribozyme. (c) Cy5 channel showing uptake of Cy5-labeled ribozyme−SNAs into T98G cells. (d) Bright-field image with Cy5 channel overlay of T98G cells post treatment with Cy5-labeled ribozyme−SNAs. No transfection agents were used for either free Cy5-ribozymes or Cy5-ribozyme−SNAs. Scale bar is 20 μm.

As the cellular environment is rich in nucleolytic enzymes, a major concern is the prolonged stability of the ribozyme. Since the ribozymes used in this study are unmodified, we investigated whether the SNA could shield or protect the ribozymes from degradation, as previously observed for siRNA− and DNA−SNAs.[28,29] To study this, an assay

DOI: 10.1021/jacs.5b07104
J. Am. Chem. Soc. 2015, 137, 10528−10531

consisting of reverse transcription followed by PCR (RT-PCR) was developed to determine the relative stability of the ribozyme pre and post exposure to serum nucleases. The ribozyme−SNAs were incubated with 40% fetal bovine serum (FBS) for 1 h at 37 °C in an effort to expose the ribozymes to nuclease-mediated cleavage. The particles were then washed and subjected to the RT-PCR assay. PCR amplification of the full-length ribozyme was present on the SNA surface despite exposure to relatively harsh enzymatic cocktails containing common nucleases (Figure S1).

Once it was confirmed that the ribozyme's function was retained after ligation to the SNA, and that the SNA architecture conferred enhanced uptake and stability, the ribozyme−SNAs were assessed for their ability to knock down MGMT protein expression in glioma cells. The extent of MGMT knockdown was assessed via Western blot analysis. Ribozyme−SNAs were incubated with T98G glioma cells overnight, and protein lysates were harvested for immunoblotting after 48−96 h. Representative gels are shown in Figure 4, along with the averaged results quantified by densitometry (n = 3).

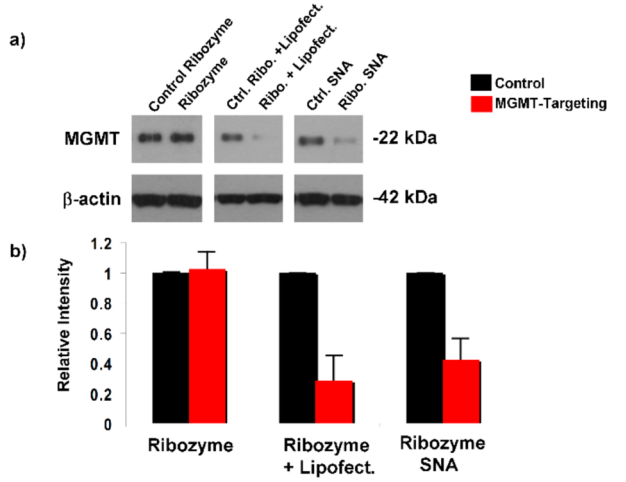

Figure 4. Silencing of MGMT by ribozyme−SNAs. (a) T98G cells were treated with control or MGMT-targeting free ribozyme, free ribozyme combined with lipofectamine (LP), or ribozyme−SNAs, and the effects on MGMT protein levels were investigated by Western blots. (b) Quantification of MGMT expression by densitometric analysis (n = 3).

Treatment with the MGMT-targeting ribozyme−SNAs resulted in over 75% knockdown of MGMT protein without transfection agents. After testing the degree of MGMT knockdown, the ribozyme−SNAs were evaluated for their ability to amplify apoptotic responses to TMZ treatment. To this end, we determined effector caspase-3/7 activation and activity by a DEVDase assay (using the caspase-3/7 peptidyl substrate Ac-DEVD-AMC; BioVision, Milpitas, CA) and Western blot analysis using antibodies specific for active caspase-3 and caspase-7. Lysates from ribozyme−SNA-treated glioma cells showed a considerable increase in DEVDase activity and effector caspase activation when compared to both the transfected free ribozyme and the control ribozyme−SNA (Figure 5).

In summary, we have prepared a novel ribozyme−SNA that exhibits the ability to transfect cell membranes and retain its enzymatic activity, once inside cells. The approach and

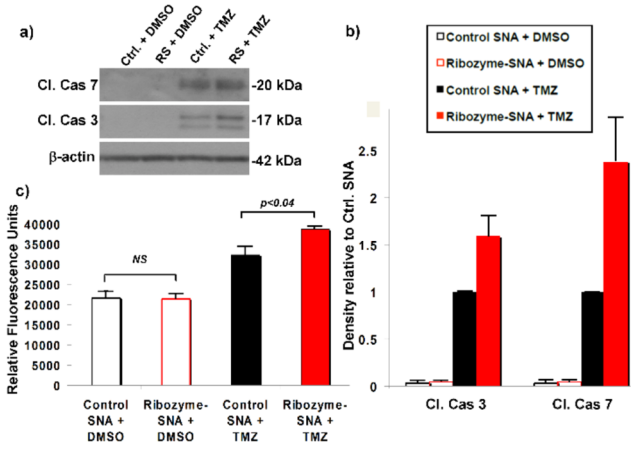

Figure 5. Caspase activation and activity triggered by ribozyme−SNAs. (a) Representative Western blot analysis showing the ability of ribozyme−SNAs to activate effector caspases-3/7 as seen by cleavage (Cl.) of either caspase. (b) Averaged caspase activation for control SNAs versus MGMT-targeting ribozyme−SNAs with TMZ treatment in T98G cells via Western blot. Ribozyme−SNAs considerably increased caspase activation relative to the control SNAs. (c) Quantification of caspase activation by ribozyme−SNAs in the presence of TMZ compared to control SNAs using a fluorescent peptide reporter assay. TMZ is dissolved in DMSO for all experiments.

chemical architecture bypass the need for chemical modifications to the RNA or external transfection agents, both of which limit conventional ribozyme utility. Importantly, the SNA architecture maintains an external environment conducive to retaining ribozyme functionality and enhances the stability of traditionally unstable nucleic acids. Furthermore, the observation that ribozyme−SNAs can effectively knock down MGMT in GBM cells and subsequently sensitize these cells to TMZ-mediated apoptosis bodes well for developing such structures as experimental therapies for GBM. Such biological results, including the ability to target and knockdown a central DNA repair protein and chemoresistance mechanism, provide functional confirmation of the structural advantages afforded by the SNA architecture. Taken together, this study suggests that enzymatic assembly of RNA on SNAs can be extended to larger, highly structured RNAs as a way to retain their native function, an essential factor in the design of nucleic acid-based therapeutics.

■ ASSOCIATED CONTENT

Supporting Information

The Supporting Information is available free of charge on the ACS Publications website at DOI: 10.1021/jacs.5b07104.

All experimental details, along with all DNA and RNA sequences (PDF)

■ AUTHOR INFORMATION

Corresponding Author

*chadnano@northwestern.edu

Author Contributions

#J.L.R. and T.L.S. contributed equally.

Notes

The authors declare no competing financial interest.

DOI: 10.1021/jacs.5b07104
J. Am. Chem. Soc. 2015, 137, 10528−10531

■ ACKNOWLEDGMENTS

This research was supported by the Center for Cancer Nanotechnology Excellence (CCNE) initiative of the National Institutes of Health (NIH) under Award U54 CA151880, the National Institute of Arthritis and Musculoskeletal and Skin Diseases Award R01AR060810, the Defense Advanced Research Projects Agency Grant HR0011-13-2-0018, and the John McNicholas Foundation. J.L.R. acknowledges a Postdoctoral Fellowship in Pharmaceutics from the Pharmaceutical Research and Manufacturers of America Foundation. L.H. acknowledges a Howard Hughes Medical Institute International Predoctoral Fellowship. T.L.S. acknowledges the National Cancer Institute/National Institutes of Health NRSA Fellowship Award F30CA174058-01. T.L.S. and L.H. gratefully acknowledge support from a Ryan Fellowship. All confocal analysis was performed at the Quantitative Bio-element Imaging Center at Northwestern University.

■ REFERENCES

(1) Kruger, K.; Grabowski, P. J.; Zaug, A. J.; Sands, J.; Gottschling, D. E.; Cech, T. R. *Cell* **1982**, *31*, 147.
(2) Symons, R. H. *Curr. Opin. Struct. Biol.* **1994**, *4*, 322.
(3) Dawson, P. A.; Marini, J. C. *Nucleic Acids Res.* **2000**, *28*, 4013.
(4) Ellis, J.; Rogers, J. *Nucleic Acids Res.* **1993**, *21*, 5171.
(5) Citti, L.; Rainaldi, G. *Curr. Gene Ther.* **2005**, *5*, 11.
(6) Burnett, J. C.; Rossi, J. J. *Chem. Biol.* **2012**, *19*, 60.
(7) Brus, C.; Petersen, H.; Aigner, A.; Czubayko, F.; Kissel, T. *Bioconjugate Chem.* **2004**, *15*, 677.
(8) Shu, Y.; Shu, D.; Haque, F.; Guo, P. *Nat. Protoc.* **2013**, *8*, 1635.
(9) Bai, Y.; Li, H.; Vu, G.-P.; Gong, H.; Umamoto, S.; Zhou, T.; Lu, S.; Liu, F. *Proc. Natl. Acad. Sci. U. S. A.* **2010**, *107*, 7269.
(10) Hughes, M. D.; Hussain, M.; Nawaz, Q.; Sayyed, P.; Akhtar, S. *Drug Discovery Today* **2001**, *6*, 303.
(11) Klopffer, A. E.; Engels, J. W. *Nucleosides, Nucleotides Nucleic Acids* **2003**, *22*, 1347.
(12) Christiansen, J. K.; Lobedanz, S.; Arar, K.; Wengel, J.; Vester, B. *Bioorg. Med. Chem.* **2007**, *15*, 6135.
(13) Wang, Z.; Liu, H.; Yang, S. H.; Wang, T.; Liu, C.; Cao, Y. C. *Proc. Natl. Acad. Sci. U. S. A.* **2012**, *109*, 12387.
(14) Rosi, N. L.; Giljohann, D. A.; Thaxton, C. S.; Lytton-Jean, A.; Han, M. S.; Mirkin, C. A. *Science* **2006**, *312*, 1027.
(15) Patel, P. C.; Hao, L.; AuYeung, W. S.; Mirkin, C. A. *Mol. Pharmaceutics* **2011**, *8*, 1285.
(16) Morris, W.; Briley, W. E.; Auyeung, E.; Cabezas, M. D.; Mirkin, C. A. *J. Am. Chem. Soc.* **2014**, *136*, 7261.
(17) Banga, R. J.; Chernyak, N.; Narayan, S. P.; Nguyen, S. T.; Mirkin, C. A. *J. Am. Chem. Soc.* **2014**, *136*, 9866.
(18) Rouge, J. L.; Hao, L.; Wu, X. A.; Briley, W. E.; Mirkin, C. A. *ACS Nano* **2014**, *8*, 8837.
(19) Prado-Gotor, R.; Grueso, E. *Phys. Chem. Chem. Phys.* **2011**, *13*, 1479.
(20) Ivanov, S.; Alekseev, Y.; Bertrand, J.-R.; Malvy, C.; Gottikh, M. B. *Nucleic Acid Res.* **2003**, *31*, 4256.
(21) Cutler, J. I.; Zhang, K.; Zheng, D.; Auyeung, E.; Prigodich, A. E.; Mirkin, C. A. *J. Am. Chem. Soc.* **2011**, *133*, 9254.
(22) Sharma, S.; Salehi, F.; Scheithauer, B. W.; Rotondo, F.; Syro, L. V.; Kovacs, K. *Anticancer Res.* **2009**, *29*, 3759.
(23) Lechapt-Zalcman, E.; Levallet, G.; Dugue, A. E.; Diebold, M. D.; Colin, P.; Peruzzy, P.; Emery, E.; Bernaudin, M.; Chapon, F.; Guillamo, J. S. *Cancer* **2012**, *118*, 4545.
(24) Hegi, M.; Diserens, A.-C.; Gorlia, T.; Hamou, M.-F.; de Tribolet, N.; Weller, M.; Kros, J. M.; Hainfellner, J. A.; Mason, W.; Mariani, L.; Bromberg, J. E. C.; Hau, P.; Mirimanoff, R. O.; Cairncross, J. G.; Janzer, R. C.; Stupp, R. *N. Engl. J. Med.* **2005**, *352*, 997.
(25) Krex, D.; Klink, B.; Hartmann, C.; von Deimling, A.; Pietsch, T.; Simon, M.; Steinback, J. P.; Heese, O.; Reifenberger, G.; Weller, M.; Schackert, G. *Brain* **2007**, *130*, 2596.
(26) Citti, L.; Eckstein, F.; Capecchi, B.; Mariani, L.; Nevischi, S.; Poggi, A.; Rainaldi, G. *Antisense Nucleic Acid Drug Dev.* **1999**, *9*, 125.
(27) Hendry, P.; McCall, M. J.; Stewart, T. S.; Lockett, T. J. *BMC Chem. Biol.* **2004**, *4*, 1.
(28) Barnaby, S. N.; Lee, A.; Mirkin, C. A. *Proc. Natl. Acad. Sci. U. S. A.* **2014**, *111*, 9739.
(29) Cutler, J. I.; Auyeung, E.; Mirkin, C. A. *J. Am. Chem. Soc.* **2012**, *134*, 1376.

DOI: 10.1021/jacs.5b07104
J. Am. Chem. Soc. 2015, 137, 10528−10531